Neuron, Vol. 33, 115–122, January 3, 2002, Copyright ©2002 by Cell Press

Bradykinin and ATP Accelerate Ca^{2+} Efflux from Rat Sensory Neurons via Protein Kinase C and the Plasma Membrane Ca^{2+} Pump Isoform 4

Yuriy M. Usachev,[1] Steven J. DeMarco,[2] Colin Campbell,[1] Emanuel E. Strehler,[2] and Stanley A. Thayer[1,3]
[1] Department of Pharmacology
University of Minnesota
6-120 Jackson Hall
321 Church Street SE
Minneapolis, Minnesota 55455
[2] Department of Biochemistry and Molecular Biology
Mayo Graduate School
Mayo Clinic
200 First Street SW
Rochester, Minnesota 55905

Summary

Modulation of Ca^{2+} channels by neurotransmitters provides critical control of neuronal excitability and synaptic strength. Little is known about regulation of the Ca^{2+} efflux pathways that counterbalance Ca^{2+} influx in neurons. We demonstrate that bradykinin and ATP significantly facilitate removal of action potential-induced Ca^{2+} loads by stimulating plasma membrane Ca^{2+}-ATPases (PMCAs) in rat sensory neurons. This effect was mimicked in the soma and axonal varicosities by phorbol esters and was blocked by antagonists of protein kinase C (PKC). Reduced expression of PMCA isoform 4 abolished, and overexpression of isoform 4b enhanced, PKC-dependent facilitation of Ca^{2+} efflux. This acceleration of PMCA4 underlies the shortening of the action potential afterhyperpolarization produced by activation of bradykinin and purinergic receptors. Thus, isoform-specific modulation of PMCA-mediated Ca^{2+} efflux represents a novel mechanism to control excitability in sensory neurons.

Introduction

Intracellular Ca^{2+} concentration ($[Ca^{2+}]_i$) controls a number of neuronal functions, including excitability, neurotransmitter release, gene expression, and neurotoxicity (Ghosh and Greenberg, 1995). Ca^{2+} entering the cell during excitation must be efficiently removed from the cytoplasm to maintain normal Ca^{2+} homeostasis. The plasma membrane Ca^{2+}-ATPases (PMCAs) are key components of the Ca^{2+} extrusion machinery in neurons (Miller, 1991). The four PMCA gene products are heterogeneously distributed in brain and are present in the soma, presynaptic terminals, dendrites, and dendritic spines (Carafoli, 1994; Filoteo et al., 1997; Juhaszova et al., 2000; Stauffer et al., 1995). The high affinity of PMCAs for Ca^{2+} (0.2–0.6 μM) (Wang et al., 1992) and their colocalization with voltage-gated Ca^{2+} channels (Hillman et al., 1996) make these pumps ideally suited to lower $[Ca^{2+}]_i$ following bursts of electrical activity.

[3] Correspondence: thayer@med.umn.edu

PMCAs play a special role in sensory function. They are the primary mechanism for Ca^{2+} expulsion from the somata of dorsal root ganglion (DRG) neurons (Benham et al., 1992; Werth et al., 1996) and from the presynaptic terminals of photoreceptors (Krizaj and Copenhagen, 1998) and retinal bipolar neurons (Zenisek and Matthews, 2000). PMCA2 extrudes Ca^{2+} from hair cell stereocilia (Yamoah et al., 1998), and inactivation of the PMCA2 gene in mice is associated with balance and hearing deficits (Kozel et al., 1998; Street et al., 1998).

The carboxy-terminal domains of PMCAs can be phosphorylated by protein kinase A (PKA) and protein kinase C (PKC) (Kosk-Kosicka and Zylinska, 1997; Wang et al., 1992). The site of phosphorylation varies among PMCA isoforms, and alternative splicing of primary transcripts alters its presence and position (Strehler and Zacharias, 2001). Thus, neuromodulators that stimulate PKA or PKC are predicted to modify PMCA-mediated Ca^{2+} transport in an isoform-specific manner, although this idea has not previously been tested.

Bradykinin is a potent pain-producing peptide that is generated at sites of tissue damage and inflammation (Dray and Perkins, 1993). ATP is a key neurotransmitter in the sensory nervous system involved in the transduction of pain and proprioception (Cook et al., 1997; Nakamura and Strittmatter, 1996). Both bradykinin and ATP control excitability in sensory neurons through mechanisms that are not fully understood. These agonists activate metabotropic receptors that couple to phospholipase C (Burgess et al., 1989; Ralevic and Burnstock, 1998; Thayer et al., 1988). Because bradykinin and ATP stimulate PKC-dependent pathways and PMCAs are potentially phosphorylated by PKC, we tested the hypothesis that bradykinin and ATP would modulate Ca^{2+} efflux in DRG neurons.

We found that these neuromodulators accelerated Ca^{2+} efflux via PKC in a manner that was dependent on the expression of a particular PMCA isoform. Bradykinin and an ATP analog reduced the duration of the action potential afterhyperpolarization (AHP) by facilitating PMCA-mediated Ca^{2+} efflux. Therefore, modulation of PMCAs by neurotransmitters and neuroactive peptides participates in the control of neuronal excitability.

Results

PMCA-Mediated Ca^{2+} Efflux in Rat DRG Neurons

In DRG neurons, high affinity Ca^{2+} pumps of the endoplasmic reticulum and plasma membrane are the principal mechanisms that control $[Ca^{2+}]_i$ recovery to basal levels after small Ca^{2+} loads (Benham et al., 1992; Usachev and Thayer, 1999; Werth et al., 1996). Monitoring PMCA-mediated Ca^{2+} efflux is hampered by the absence of selective inhibitors and a relatively low turnover rate of the pump, making electrophysiological detection of this transport unfeasible. PMCA-mediated Ca^{2+} efflux from DRG somata was studied in isolation by limiting the size of the $[Ca^{2+}]_i$ increase to less than 350 nM and by blocking the sarco-endoplasmic reticulum Ca^{2+}-

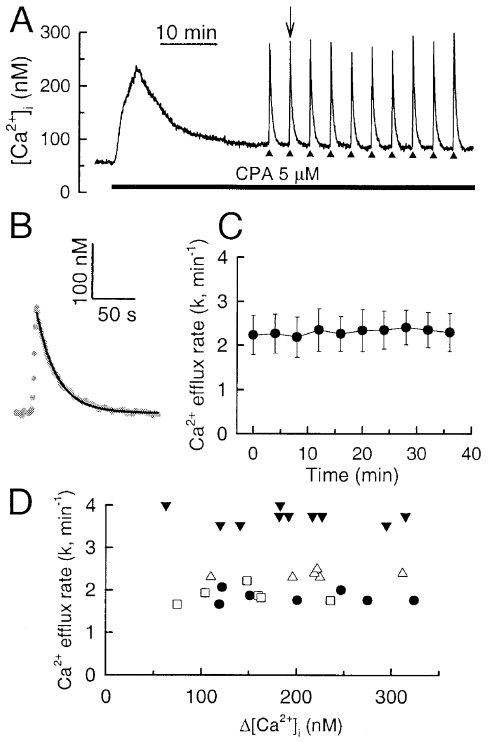

Figure 1. The Rate of Ca^{2+} Efflux in DRG Neurons Remains Stable during the Recording and Is Independent of the Amplitude of the $[Ca^{2+}]_i$ Response

(A) A protocol for studying PMCA-mediated $[Ca^{2+}]_i$ recovery kinetics. $[Ca^{2+}]_i$ was recorded as described in Experimental Procedures. CPA (horizontal bar) and electric field stimulation (4 s, 8 Hz; black arrowheads) were applied at the times indicated.

(B) The $[Ca^{2+}]_i$ transient indicated by the vertical arrow in (A) is displayed (dotted line) on an expanded time scale. The recovery phase of the $[Ca^{2+}]_i$ response was fit with a monoexponential function (solid line) as described in Experimental Procedures.

(C) Rate constants obtained from five independent experiments such as those described in (A) were averaged and plotted versus time (mean ± SEM). The first stimulation was at time 0.

(D) Rate constants are plotted versus the amplitude of the corresponding $[Ca^{2+}]_i$ increase for four individual cells. Each neuron is represented by a unique symbol.

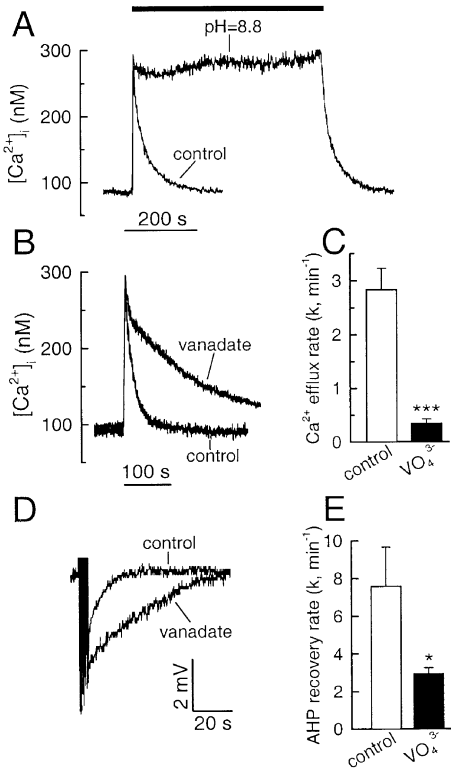

Figure 2. Elevated Extracellular pH and Vanadate Inhibit Ca^{2+} Efflux and Prolong the Action Potential AHP in DRG Neurons

(A) The effect of extracellular pH was studied in DRG neurons loaded with indo-1 AM. $[Ca^{2+}]_i$ transients were elicited using extracellular field stimulation in the presence of 5 μM CPA. Two $[Ca^{2+}]_i$ responses obtained from the same cell are superimposed. The control trace was recorded at normal pH (7.35). Increasing extracellular pH to 8.8 (horizontal bar) blocked $[Ca^{2+}]_i$ recovery in five of eight cells tested and greatly slowed it in the other three cells. Return to pH 7.35 restored the recovery process.

(B) $[Ca^{2+}]_i$ measurements were combined with patch-clamp recording using the current-clamp configuration. Small Ca^{2+} loads were elicited by brief trains of action potentials in the presence of 5 μM CPA. A control $[Ca^{2+}]_i$ trace is superimposed with one obtained from a cell with 200 μM Na_3VO_4 added to the pipette solution.

(C) Bar graph summarizes rate constants obtained from 12 control cells and 10 cells treated with VO_4^{3-} as described in (B). (***$p < 0.001$, unpaired Student's t test.)

(D) AHPs following a burst of action potentials in the absence and presence of vanadate are compared. Voltage traces were obtained in the presence of 5 μM CPA using the current-clamp mode. Action potential amplitude was truncated. Introduction of 200 μM VO_4^{3-} through the patch pipette markedly slowed recovery of the AHP.

(E) Bar graph summarizes the AHP recovery rate from 12 control cells and 10 cells treated with VO_4^{3-} as described in (D). The recovery of the AHP was fit with a monoexponential function as described in Experimental Procedures. (*$p < 0.05$, unpaired Student's t test.)

ATPase (SERCA) with 5 μM cyclopiazonic acid (CPA) (Thomas and Hanley, 1994). CPA evoked a transient elevation in $[Ca^{2+}]_i$ from 58 ± 3 to 204 ± 10 nM ($n = 25$; Figure 1A) that recovered to a new steady-state level of 73 ± 5 nM ($n = 25$) within 10–25 min. Thus, PMCA-mediated Ca^{2+} efflux was studied 30 min after CPA treatment. Transient $[Ca^{2+}]_i$ elevations were elicited every 4 min by brief trains of action potentials (3–5 s, 5–10 Hz) using extracellular field stimulation (Figure 1A). $[Ca^{2+}]_i$ recovery was well described by a monoexponential function (correlation coefficient > 0.97; Figure 1B). The rate constant (k), a value reciprocal to the time constant, was calculated for each $[Ca^{2+}]_i$ transient and used as an index of Ca^{2+} efflux rate. The rate of Ca^{2+} efflux was stable throughout the experiment; k was 2.2 ± 0.4 min^{-1} for the first $[Ca^{2+}]_i$ response and 2.3 ± 0.4 min^{-1} ($n = 5$) for the tenth response 36 min later. The rate of Ca^{2+} efflux was not influenced by the size of the Ca^{2+} load applied in this study (range 50–350 nM) (Figure 1D).

To verify that the rate of $[Ca^{2+}]_i$ recovery in this paradigm was predominantly controlled by PMCA activity, we inhibited PMCA function and then recorded the effect on $[Ca^{2+}]_i$ recovery kinetics. Ca^{2+} transport by PMCAs requires counter-transport of protons and thus is inhibited by raising external pH (Benham et al., 1992; Schwiening et al., 1993). $[Ca^{2+}]_i$ recovery in DRG neurons was dramatically slowed at pH 8.8 (Figure 2A). Vanadate acts on an intracellular site of the PMCA to inhibit Ca^{2+}

transport (Carafoli, 1994). $[Ca^{2+}]_i$ recording was combined with the whole-cell patch-clamp technique to test the effect of vanadate on Ca^{2+} efflux. $[Ca^{2+}]_i$ transients recorded under these conditions (Figure 2B) were similar ($k = 2.8 \pm 0.4$ min^{-1}; $n = 12$) to those obtained from intact cells. Addition of 200 μM Na^+-orthovanadate to the pipette solution resulted in a more than 9-fold slowing of Ca^{2+} efflux (Figures 2B and 2C), so that the rate constant decreased to 0.3 ± 0.1 min^{-1} ($n = 10$).

To determine whether PMCAs participate in the control of membrane excitability, we studied the effects of vanadate on the action potential AHP. The slow AHP is produced by Ca^{2+}-activated K^+ channels in DRG neurons (Sah, 1996) and, therefore, is tightly linked to intracellular Ca^{2+} homeostasis. Following a train of action potentials, 68% ($n = 31$) of DRG neurons displayed a slow AHP. As shown in Figures 2D and 2E, 200 μM Na^+-orthovanadate significantly decreased the AHP recovery rate in DRG neurons (7.6 ± 2.1 min^{-1} in control [$n = 12$] and 2.9 ± 0.3 min^{-1} in vanadate-treated cells [$n = 10$]). Thus, PMCA-mediated Ca^{2+} efflux controls the duration of the slow AHP.

The recovery kinetics for the small Ca^{2+} loads used in this study were not influenced by Na^+/Ca^{2+} exchange or mitochondrial Ca^{2+} uptake. $[Ca^{2+}]_i$ transients evoked by depolarization (−60 to +10 mV, 10 ms, 10 Hz) in the whole-cell configuration of the patch clamp had similar recovery rates in Na^+-containing ($k = 2.2 \pm 0.2$ min^{-1}; $n = 5$) and Na^+-free solution (2.3 ± 0.5 min^{-1}; $n = 5$) (data not shown). Elevating intracellular Na^+ with 200 μM ouabain was also without effect on recovery from action potential-induced Ca^{2+} loads in intact cells ($n = 6$). Treating cells with mitochondrial poisons blocks mitochondria-mediated Ca^{2+} buffering of large Ca^{2+} loads (Werth and Thayer, 1994), but did not alter $[Ca^{2+}]_i$ recovery kinetics in the field stimulation paradigm used here. The rate constant was 2.2 ± 0.4 min^{-1} ($n = 6$) before and 2.3 ± 0.3 min^{-1} ($n = 6$) after treatment with carbonyl cyanide p-trifluomethoxy phenyl hydrazone (FCCP; 1 μM) and oligomycin B (10 μM). Thus, with SERCAs blocked, PMCA-mediated Ca^{2+} efflux was the dominant mechanism that determined $[Ca^{2+}]_i$ recovery kinetics in DRG neurons following small Ca^{2+} loads.

Stimulation of PKC Accelerates Ca^{2+} Efflux

Having established a paradigm to measure PMCA-mediated Ca^{2+} efflux, we next examined the effects of PKA and PKC activation on $[Ca^{2+}]_i$ recovery kinetics. After 30 min in CPA, four action potential-induced increases in $[Ca^{2+}]_i$ were elicited to establish control recovery kinetics (Figure 3A). Activation of PKA by treating cells with membrane permeant analogs of cyclic AMP (1 mM 8-Br-cAMP [$n = 8$] or 100 μM pCPT-cAMP [$n = 6$]) did not affect the rate of Ca^{2+} efflux (data not shown). In contrast, activation of PKC using 0.5 μM phorbol-12,13-dibutyrate (PDBu) markedly accelerated the $[Ca^{2+}]_i$ recovery process (Figure 3). Because the rate constant of Ca^{2+} efflux varied substantially among DRG neurons (range, 1–4 min^{-1}), in order to pool data from multiple cells, the rate constant for each $[Ca^{2+}]_i$ transient was normalized to that calculated for the first (control) transient for each cell. After treatment with PDBu for 24 min, the rate constant reached 146% ± 5% of control ($n =$ 14). The effect of PDBu was maximal because increasing the concentration to 2 μM produced a comparable increase in the rate of Ca^{2+} efflux ($k = 143\% \pm 5\%$ of control; $n = 3$). The effect of PDBu was blocked completely by the selective PKC antagonists GF109203x (5 μM; $n = 5$) or Ro31-8220 (2 μM; $n = 4$) (Figure 3C). The antagonists did not significantly affect the basal rate of Ca^{2+} efflux, and the potentiation of Ca^{2+} efflux did not correlate with the initial rate constant. Phorbol-12-myristate-13-acetate (PMA, 1 μM), but not its inactive analog 4-α-PMA (1 μM), also substantially increased the rate

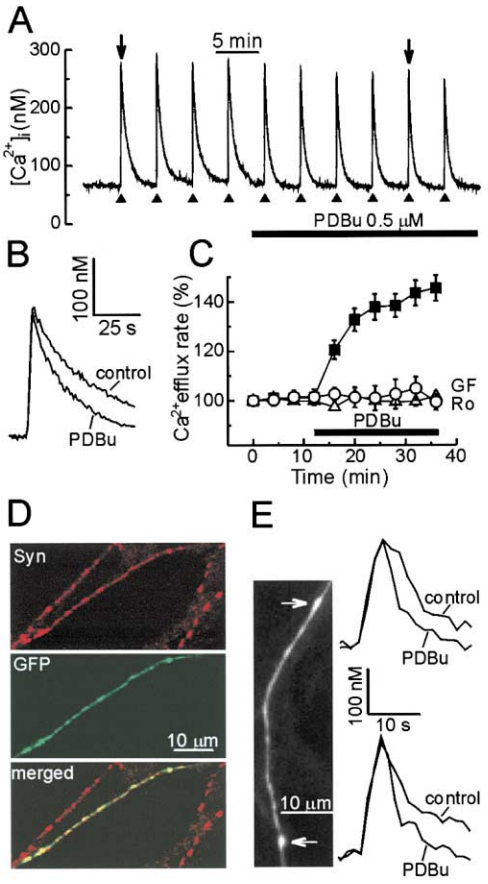

Figure 3. Stimulation of PKC Facilitates Ca^{2+} Efflux

(A) Representative recording of $[Ca^{2+}]_i$ before and during treatment with 0.5 μM PDBu (horizontal bar). Ca^{2+} efflux rate was studied in indo-1 AM-loaded DRG neurons. Small Ca^{2+} loads were elicited every 4 min in CPA-treated cells (5 μM) using extracellular field stimulation.

(B) $[Ca^{2+}]_i$ responses recorded before (control) and after treatment with PDBu (vertical arrows in [A]) are superimposed on an expanded time scale.

(C) The effect of 0.5 μM PDBu (horizontal bar) on the normalized rate constant is summarized for 14 cells (■). The PDBu-induced stimulation of Ca^{2+} efflux was completely blocked by 5 μM GF109203x (GF, △) or 2 μM Ro31-8220 (Ro, ○) (for $t \geq 20$ min, $p < 0.001$, one-way ANOVA with Bonferroni post hoc test). PKC antagonists were applied 30 min prior to the first field stimulation.

(D) Axonal varicosities were studied in DRG-spinal neuron cocultures. Synaptophysin (Syn) immunoreactivity was present in the varicosities of a GFP-expressing neuron as evident in the merged image.

(E) $[Ca^{2+}]_i$ was recorded from the fura-2-loaded axon shown. $[Ca^{2+}]_i$ responses from the varicosities identified by the arrows are shown before and after 10 min treatment with 0.5 μM PDBu.

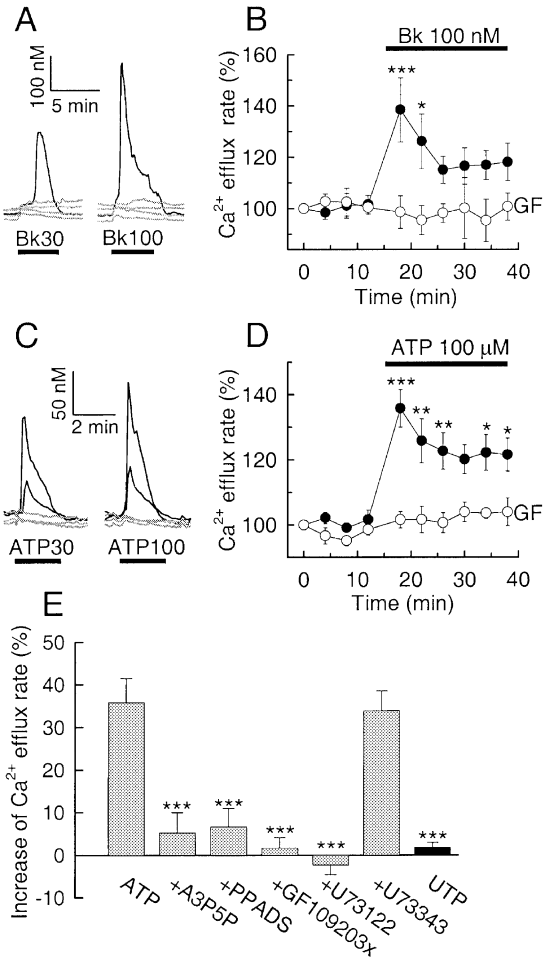

Figure 4. Bradykinin and ATP Accelerate Ca^{2+} Efflux from DRG Neurons

(A) $[Ca^{2+}]_i$ was recorded with fura-2-based digital imaging from small (<21 μm) DRG neurons cultured for 2–7 days. The horizontal bars indicate application of 30 or 100 nM bradykinin. The break between the recordings corresponds to 20 min. A cell was considered responsive if 30 nM bradykinin evoked an increase in $[Ca^{2+}]_i$ that was both greater than 100 nM and at least 50% above baseline (Stucky et al., 1996). In the experiment shown, one of five cells responded to bradykinin (black line).

(B) The normalized rate constant was plotted versus time for responsive cells before and during 100 nM bradykinin treatment (horizontal bar). All recordings were performed in the presence of 5 μM CPA. Application of bradykinin started 2 min prior to subsequent field stimulation. Bradykinin significantly accelerated the rate of Ca^{2+} efflux (●; n = 6), an effect blocked by GF109203x (GF, 2 μM, ○; n = 5). GF109203x and CPA were applied simultaneously (t = −30 min). (***p < 0.001, *p < 0.05, one-way ANOVA, Bonferroni post hoc test.)

(C) 30 or 100 μM ATP was applied to fura-2 AM-loaded cells as indicated by horizontal bars. Neurons were placed in Ca^{2+}-free solution during ATP treatment. The break between the recordings corresponds to 25 min. The same criteria as those described in (A) were used to distinguish responsive (black line) from nonresponsive (gray line) cells.

(D) The normalized rate constant was plotted versus time before and during ATP treatment (horizontal bar). ATP significantly increased the rate of Ca^{2+} efflux in control cells (●; n = 8), but not in cells treated with 2 μM GF109203x (GF, ○; n = 5). ATP application began 2 min prior to field stimulation. GF109203x and CPA were applied simultaneously (t = −30 min). (*p < 0.05, **p < 0.01, ***p < 0.001, one-way ANOVA with Bonferroni post hoc test.)

of Ca^{2+} efflux. After 24 min of treatment with PMA, the rate constant reached 140% ± 8% of control (n = 5), whereas for 4-α-PMA it was 104% ± 3% of control (n = 5). Although most recordings were obtained in young DRG neurons (2–3 days in culture), we found a similar PKC-dependent facilitation of Ca^{2+} efflux (k = 161% ± 12% of control; n = 7) in 14- to 18-day-old cultures.

Activation of PKC also accelerated $[Ca^{2+}]_i$ recovery in DRG axons as indicated by fura-2-based digital imaging. Varicosities on sensory axons release neurotransmitters and neuropeptides (Kessler et al., 1999), consistent with the synaptophysin immunoreactivity present in these structures (Figure 3D). PDBu (0.5 μM) increased the rate of recovery from action potential-induced increases in $[Ca^{2+}]_i$ recorded from these release sites (Figure 3E). The rate constant increased to 179% ± 25% of control (n = 14 varicosities from four cells). The acceleration of Ca^{2+} efflux was inhibited completely by 5 μM GF109203x (n = 9 varicosities from three cells; $p < 0.05$, Student's t test).

ATP and Bradykinin Induce PKC-Dependent Facilitation of Ca^{2+} Efflux

Because activation of PKC by phorbol esters accelerated Ca^{2+} efflux, we hypothesized that neurotransmitters or neuropeptides that activate phospholipase C would elicit similar effects. A subset of DRG neurons expresses receptors for bradykinin that, when activated, stimulate the production of diacylglycerol (DAG) with subsequent activation of PKC (Burgess et al., 1989; Cesare et al., 1999; Thayer et al., 1988). Therefore, we determined whether bradykinin accelerates Ca^{2+} extrusion from DRG neurons. In each experiment, bradykinin was applied twice. The first application was used to identify a responsive cell by monitoring bradykinin-induced Ca^{2+} mobilization (Stucky et al., 1996). The second treatment examined the effect of bradykinin on the Ca^{2+} efflux rate in a responsive cell. To minimize desensitization of bradykinin receptors (Dray and Perkins, 1993), a submaximal concentration of bradykinin (30 nM) was used for the first application and a saturating concentration (100 nM) for the second. As shown in Figure 4A, when bradykinin applications were separated by a 30 min wash period, 100 nM bradykinin produced a robust response. Responsive cells were washed for 30 min, treated with 5 μM CPA, and then four action potential-induced $[Ca^{2+}]_i$ transients were evoked to determine the Ca^{2+} efflux rate under these control conditions. In the presence of CPA, bradykinin-evoked $[Ca^{2+}]_i$ responses, if present, were small (<50 nM) and brief (<1 min), consistent with release from inositol 1,4,5-trisphosphate (IP_3)-sensitive stores as the main Ca^{2+} source (Thayer et al., 1988). Bradykinin (100 nM) produced a significant acceleration of Ca^{2+} efflux that reached its maximum (k = 138% ± 12% of control; n = 6) during the first 2

(E) Pharmacology of ATP stimulated Ca^{2+} efflux. Bar graph summarizes the effects of ATP (100 μM; gray bars) and UTP (100 μM; solid bar) on Ca^{2+} efflux in the presence of the indicated antagonists (n = 4–8). Comparisons were made 2 min after agonist application using the protocol described in (D). (***p < 0.001 relative to stimulation with ATP alone, one-way ANOVA with Bonferroni post hoc test.)

min of treatment (Figure 4B). The B_2 receptor antagonist, HOE140 (0.5 μM), completely blocked the effects of bradykinin ($n = 5$; $p < 0.05$, unpaired Student's t test). The bradykinin-induced facilitation of Ca^{2+} efflux was blocked completely by 2 μM GF109203x ($n = 5$), indicating that this effect was mediated by PKC (Figure 4B). Unlike stimulation with phorbol esters, the acceleration of Ca^{2+} efflux by bradykinin was transient. This observation is in agreement with the transient activation of PKC by bradykinin in DRG neurons (Cesare et al., 1999) and likely results from receptor desensitization (Dray and Perkins, 1993).

DRG neurons express at least two types of purinergic receptors, ionotropic ($P2X_2$ and $P2X_3$) and metabotropic ($P2Y_1$) (Cook et al., 1997; Nakamura and Strittmatter, 1996). In a subset of DRG neurons, activation of $P2Y_1$ receptors stimulates PLC leading to the production of IP_3 and DAG (Ralevic and Burnstock, 1998) and the release of Ca^{2+} (Svichar et al., 1997). We hypothesized that ATP would activate PKC and facilitate Ca^{2+} efflux. To identify responsive cells, ATP (30 μM) was applied in Ca^{2+}-free medium to avoid Ca^{2+} influx as a result of activation of P2X receptors (Cook et al., 1997). Application of 100 μM ATP following a 30 min wash period produced a similar $[Ca^{2+}]_i$ response (Figure 4C). This second $[Ca^{2+}]_i$ transient was completely blocked by a 25 min pretreatment with 5 μM CPA ($n = 7$), confirming that ATP released Ca^{2+} from IP_3-sensitive Ca^{2+} stores. After finding a responsive cell and washing for 30 min, it was treated with 5 μM CPA and four control $[Ca^{2+}]_i$ transients were elicited using extracellular field stimulation (Figure 4D). ATP evoked small $[Ca^{2+}]_i$ increases (<50 nM) in 11 of 21 cells that rapidly recovered to basal levels (<1 min), suggesting that Ca^{2+} influx induced by activation of P2X receptors was relatively modest under these recording conditions. These brief $[Ca^{2+}]_i$ increases had recovered prior to applying the stimulus train and thus did not interfere with measuring $[Ca^{2+}]_i$ recovery kinetics. ATP caused a marked facilitation of Ca^{2+} efflux in DRG neurons (Figure 4D). This facilitation was transient, probably reflecting desensitization of the receptors (Ralevic and Burnstock, 1998). The maximal effect was observed after 2 min of treatment with ATP ($k = 136\% \pm 6\%$ of control; $n = 8$). The PKC antagonist GF109203x (2 μM; $n = 5$) inhibited this facilitation of Ca^{2+} efflux (Figure 4D). ATP-stimulated Ca^{2+} efflux was inhibited by the P2 receptor competitive antagonist PPADS (300 μM, $n = 5$) and the selective $P2Y_1$ receptor antagonist A3P5P (300 μM; $n = 5$) (Boyer et al., 1996), whereas UTP (100 μM) did not affect Ca^{2+} efflux kinetics ($n = 4$), consistent with ATP acting via $P2Y_1$ receptors (Ralevic and Burnstock, 1998) (Figure 4E). The ATP-induced acceleration of Ca^{2+} efflux was blocked by the PLC inhibitor U73122 (1 μM; $n = 4$), but not by its inactive analog U73343 (1 μM; $n = 4$) (Figure 4E).

PMCA4 Mediates PKC-Dependent Facilitation of Ca^{2+} Efflux

We next sought to identify the PMCA isoform responsible for PKC-dependent acceleration of Ca^{2+} efflux. Western analysis of a neuron-enriched DRG culture with isoform-specific antibodies revealed PMCA2 and PMCA4 as dominant isoforms, whereas only low levels of PMCA1 were found and PMCA3 was undetectable (Figure 5A). Based on their relative migration in SDS gels (Filoteo et al., 1997), the major alternative splice forms of PMCA2 and PMCA4 in the DRG neurons are 2a and 4b, respectively. In membrane preparations from COS cells, phosphorylation of PMCA2a by PKC prevents calmodulin binding to this isoform and therefore inhibits its activation by Ca^{2+}-calmodulin (Enyedi et al., 1997). In contrast, phosphorylation by PKC activated PMCA4b in the same preparation (Enyedi et al., 1996). Because stimulation of PKC facilitated Ca^{2+} efflux in DRG neurons, we focused on the PMCA4 isoform.

PMCA4 was distributed throughout sensory neurons. Expression of a PMCA4b-GFP fusion protein indicated a widespread distribution of GFP fluorescence, notably in axonal varicosities (Figure 5B). These varicosities labeled positive for synaptophysin, a marker for vesicular release. Similarly, labeling with antibody JA9 indicated PMCA4 immunoreactivity throughout the cell, including axonal varicosities that were positive for synaptophysin (data not shown).

We studied PKC-dependent modulation of Ca^{2+} efflux in neurons with altered expression of PMCA4. DRG neurons were cotransfected with plasmids that altered PMCA4 levels and a green fluorescent protein (GFP) reporter construct using particle-mediated gene delivery. This method does not alter the electrophysiological properties or disturb Ca^{2+} metabolism in sensory neurons (Usachev et al., 2000). As shown in Figure 5C, DRG neurons transfected with empty vector and nontransfected cells showed strong labeling with a PMCA4-specific antibody, consistent with high levels of PMCA4 in these cells. Transfection with a PMCA4 antisense expression vector (AS4) reduced PMCA4 immunoreactivity (Figure 5D). AS4 expression did not affect PMCA2 expression, as indicated by immunolabeling with isoform-specific antibody NR2 (data not shown).

Neurons transfected with empty vector responded to PKC activation with an increase in the Ca^{2+} efflux rate to $145\% \pm 8\%$ ($n = 8$) of control, in good agreement with that seen in nontransfected cells (Figure 6A). Thus, neither the expression vector nor the transfection procedure affected PKC-dependent facilitation of Ca^{2+} extrusion. Transfection with AS4 did not affect significantly the rate of Ca^{2+} efflux measured before PDBu treatment. The rate constant was $2.1 \pm 0.3\ min^{-1}$ ($n = 11$) in AS4-transfected cells versus $2.2 \pm 0.2\ min^{-1}$ ($n = 20$) in nontransfected cells ($p > 0.05$, unpaired Student's t test). However, reduced PMCA4 expression eliminated the PKC-dependent acceleration of Ca^{2+} efflux, so that the rate constant remained unchanged ($102\% \pm 9\%$ of control; $n = 11$) following 24 min treatment with 0.5 μM PDBu (Figure 6A and compare Figure 6B to 6C). Transfection with the same expression vector harboring the construct in the sense orientation did not affect PMCA4 immunoreactivity or $[Ca^{2+}]_i$ recovery kinetics ($n = 4$).

If reduced levels of PMCA4 suppressed the effect of PKC activation, then overexpression of PMCA4 could be predicted to enhance it. Because the "a" and "b" splice variants of PMCA4 differ in their carboxy-terminal phosphorylation sites (Enyedi et al., 1996; Verma et al., 1999), we generated expression constructs for both hPMCA4a and hPMCA4b and overexpressed the pro-

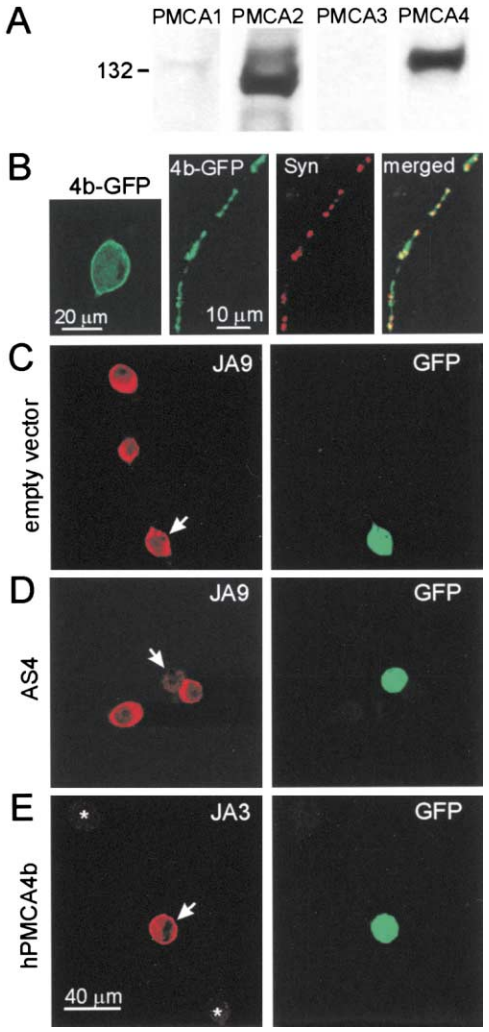

Figure 5. PMCA Isoforms in Naive and Genetically Modified DRG Neurons

(A) PMCA isoforms were analyzed on Western blots of total protein lysates obtained from neuron-enriched DRG cultures (see Experimental Procedures). 40 μg of protein was loaded in each lane. PMCA expression was analyzed using the following antibodies: NR1 for PMCA1; NR2 for PMCA2; NR3 for PMCA3; and JA9 for PMCA4 (Caride et al., 1996; Filoteo et al., 1997). The lighter band in the PMCA2 lane is likely the b splice variant. Molecular size markers are indicated in kDa on the left.

(B) Expression of a PMCA4b-GFP fusion protein produced green fluorescence in the axon and soma membranes. Axonal varicosities labeled positive for synaptophysin. Merged images show PMCA4b-GFP colocalized with synaptophysin immunoreactivity.

(C–E) DRG cultures were cotransfected with GFP and an empty vector (C), a PMCA4 antisense plasmid (AS4) (D), or a plasmid encoding hPMCA4b (E) using a "gene gun" (Usachev et al., 2000). Cells were fixed 48 hr later and labeled with PMCA4-specific antibody JA9 (C and D) or hPMCA4b-specific antibody JA3 (E). White arrows indicate transfected cells identified by GFP labeling. Human-specific antibody JA3 did not label nontransfected rat neurons (asterisks).

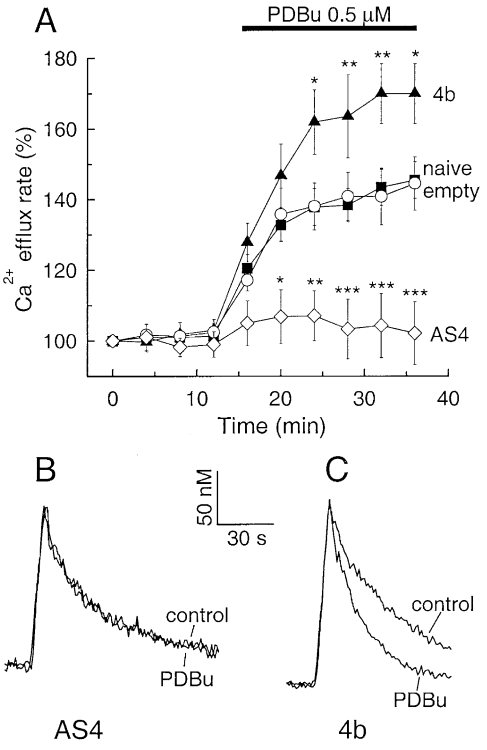

Figure 6. PKC-Dependent Facilitation of Ca^{2+} Efflux in DRG Neurons with Altered Expression of PMCA4

(A) PKC-dependent facilitation of Ca^{2+} efflux was studied as described in Figure 3. Transfected cells were identified by distinct green fluorescence 48 hr after the transfection. PDBu (0.5 μM) application (horizontal bar above the plots) produced comparable acceleration of Ca^{2+} efflux in nontransfected cells (naive, ■; n = 14) and cells transfected with an empty vector (○; n = 8). The effect of PDBu was significantly diminished in cells expressing AS4 (◇; n = 11). Cells overexpressing hPMCA4b (4b, ▲; n = 6) showed a pronounced acceleration of Ca^{2+} efflux in response to 0.5 μM PDBu. (*$p < 0.05$, **$p < 0.01$, ***$p < 0.001$, significantly different from naive cells, ANOVA with Bonferroni post hoc test.)

(B and C) Representative $[Ca^{2+}]_i$ traces from cells expressing AS4 (B) or hPMCA4b (C) before (control) and after treatment with PDBu.

teins in DRG neurons that were subsequently analyzed using the standard protocol (Figure 3A). Overexpression of hPMCA4a was confirmed using PMCA4-specific antibody JA9 (not shown), and expression of hPMCA4b was confirmed with antibody JA3, which is species (human) and splice variant specific (Figure 5E) (Caride et al., 1996). The rate constant in the absence of PDBu was 2.1 ± 0.3 min^{-1} (n = 7) for the 4a-expressing neurons and 3.0 ± 0.5 min^{-1} (n = 6) for the neurons expressing 4b. Application of 0.5 μM PDBu evoked a greater acceleration of Ca^{2+} efflux in neurons transfected with hPMCA4b than in naive cells (Figures 6A and 6C). In the 4b-expressing cells the rate constant reached 170% ± 8% of control (n = 6) after PDBu treatment, whereas in the 4a expressing cells the rate constant was comparable to control after the same treatment (n = 7; data not shown). These observations indicate that PKC-dependent acceleration of Ca^{2+} efflux in DRG neurons is mediated by PMCA4, likely its b splice variant.

Activation of Bradykinin and Purinergic Receptors Shortens the AHP via PKC-Dependent Acceleration of PMCA4

Because PMCAs control the duration of the AHP (Figures 2D and 2E), we hypothesized that PKC-dependent

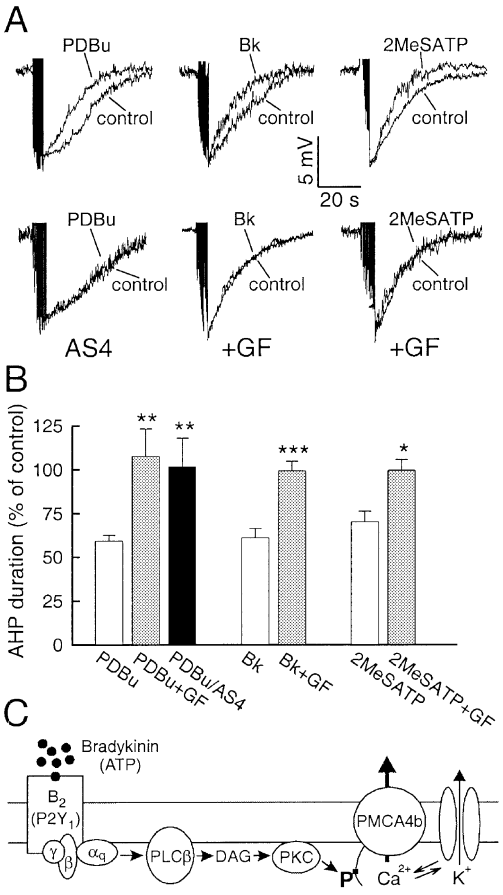

Figure 7. Activation of PKC Shortens the AHP via PMCA4

(A) Membrane potential was recorded from DRG neurons stimulated with depolarizing current injections (3–5 s, 5–10 Hz). The perforated-patch technique was used to prevent intracellular dialysis, and CPA was omitted to improve membrane stability in this configuration. Recordings from nontransfected (upper) and AS4-expressing cells (lower) are shown before (control) and 10 min after 0.5 μM PDBu. Representative AHPs are shown (upper row) before (control) and 4 min after 300 nM bradykinin (Bk) or 200 μM 2MeSATP as indicated. In the presence of 0.5 μM GF109203x (GF), agonists failed to affect the response (lower row). Agonist-responsive cells were selected using $[Ca^{2+}]_i$ imaging as described for Figure 4.

(B) Bar graph summarizes AHP recovery times normalized to the initial control response from untreated (open), GF109302x-treated (gray), and AS4-expressing (solid) cells. (*$p < 0.05$, **$p < 0.01$, ***$p < 0.001$, relative to untreated response, Student's t test.)

(C) A model for acceleration of Ca^{2+} efflux by bradykinin and ATP. Binding of bradykinin to B_2 or ATP to $P2Y_1$ receptors activates Gq and PLCβ. This leads to production of DAG and activation of PKC. PKC phosphorylates PMCA4b near the carboxyl terminus, resulting in acceleration of Ca^{2+} transport by the pump. Changes in Ca^{2+} efflux alter $[Ca^{2+}]_i$-dependent activation of K^+ channels.

facilitation of Ca^{2+} efflux would shorten the AHP. Membrane potential was recorded with the perforated patch-clamp technique, and AHPs were evoked by trains of action potentials similar to those used for Ca^{2+} efflux measurements. PDBu (0.5 μM) reduced the duration ($t_{1/2}$) of the AHP (Figures 7A and 7B) by 41% ± 3% (n = 9). This effect was completely prevented by pretreatment with 5 μM GF109203x (n = 4). PDBu did not alter the amplitude of the AHP (8 ± 1mV; n = 9), suggesting that Ca^{2+}-activated K^+ channels were not affected. In DRG neurons expressing AS4, PDBu did not affect the duration of the AHP (Figures 7A and 7B). Bradykinin (300 nM) reduced the duration of the AHP by 39% ± 5% (n = 5); this was prevented by pretreatment with GF109203x (n = 5) (Figures 7A and 7B). The $P2Y_1$ receptor agonist 2-methylthio-ATP (2MeSATP; 200 μM) reduced the duration of the AHP by 30% ± 6% (n = 5) in a GF109203x-sensitive manner (n = 4; Figures 7A and 7B). Thus, PKC-dependent acceleration of PMCA4 plays a key role in the excitation of sensory neurons by bradykinin and ATP.

Discussion

PMCAs are positioned to play a major role in the regulation of Ca^{2+} signaling in neurons. They have a high affinity for Ca^{2+}, are distributed throughout the brain, are localized to presynaptic terminals and dendritic spines, and colocalize with Ca^{2+} channels. Here we demonstrate that PMCAs are targets for the modulatory action of neurotransmitters and neuroactive peptides. Bradykinin and ATP activate PKC with subsequent acceleration of Ca^{2+} efflux from rat DRG neurons. Analysis of PKC-induced changes in $[Ca^{2+}]_i$ dynamics in neurons with altered PMCA4 expression indicated that this isoform, and specifically its splice variant b, mediated the PKC-dependent enhancement of Ca^{2+} efflux. The signaling pathway described here, metabotropic receptor activation, phosphorylation of PMCA by PKC, and an increase in the Ca^{2+} efflux rate, provides an example of what may be a general model for the modulation of $[Ca^{2+}]_i$ efflux in neurons (Figure 7C).

Activation of Metabotropic Receptors Accelerates Ca^{2+} Efflux

Bradykinin and ATP markedly accelerated Ca^{2+} efflux via a PKC-dependent pathway in DRG neurons. These results agree with an established signaling cascade in which bradykinin activation of B_2 receptors increases DAG production and activates PKC (Burgess et al., 1989; Cesare et al., 1999; Dray and Perkins, 1993; Stucky et al., 1996; Thayer et al., 1988). Similarly, our data indicate that $P2Y_1$ receptors in sensory neurons couple to phospholipase C and activate PKC. Activation of either B_2 or $P2Y_1$ receptors sensitizes DRG neurons to external stimuli by PKC-dependent phosphorylation of proteins that control excitability (Burgess et al., 1989; Dray and Perkins, 1993; Nakamura and Strittmatter, 1996; Tominaga et al., 2001). DRGs contain a heterogeneous population of neurons specialized to convey different sensory modalities and are characterized by unique electrophysiological, pharmacological, and morphological properties. Bradykinin receptors are found preferentially on small-size DRG neurons involved in nociception and characterized by immunoreactivity to substance P (Dray and Perkins, 1993; Stucky et al., 1996). $P2Y_1$ receptors are found on nociceptive and proprioceptive neurons (Nakamura and Strittmatter, 1996; Tominaga et al., 2001). Therefore, the effects of bradykinin and ATP are limited to subpopulations of sensory neurons. However, phorbol esters produced a comparable effect in DRG neurons from a broad range of sizes (15–27 μm) and ages in the culture (2–18 days). This observation implies

that PKC-dependent facilitation of Ca^{2+} efflux is a general phenomenon, typical for the majority of sensory neurons.

PMCA Isoform Diversity Produces Functional Specialization

Alternative splicing of PMCA transcripts generates Ca^{2+} pumps with diverse regulatory properties (Strehler and Zacharias, 2001). PKC-induced facilitation of PMCA-mediated Ca^{2+} efflux was previously described for endothelial cells (Wang et al., 1991) and Jurkat T cells (Balasubramanyam and Gardner, 1995), although the specific PMCA isoform responsible for this effect was not identified. Here we identify the PMCA isoform that is responsible for this facilitation in an intact cell. Knockdown of the PMCA4 isoform virtually eliminated PKC-dependent facilitation of Ca^{2+} efflux. In contrast, overexpression of the b but not the a splice variant of PMCA4 enhanced the stimulatory effect of PDBu on Ca^{2+} efflux. Thus, PMCA4b is a molecular target for PKC following activation by bradykinin or ATP in DRG neurons. In agreement with this, the 4b splice variant is one of the major PMCA isoforms expressed endogenously in DRG neurons. Our results are also in good agreement with those obtained from membrane preparations from COS cells overexpressing PMCA4a or PMCA4b (Enyedi et al., 1996; Verma et al., 1999). PKC phosphorylates the a variants of PMCA2, PMCA3, and PMCA4 within the calmodulin binding domain (Enyedi et al., 1997; Verma et al., 1999). Phosphorylation of PMCA2a and PMCA3a by PKC prevents binding of calmodulin and, therefore, activation of these isoforms (Enyedi et al., 1997), whereas phosphorylation of PMCA4a appears to be without consequence for its basal activity or calmodulin stimulation (Verma et al., 1999). In contrast, PKC phosphorylates PMCA4b at a site downstream from the calmodulin binding domain and enhances Ca^{2+} pump activity (Enyedi et al., 1996). Clearly, the specific expression pattern of PMCA variants determines the net effect of phosphorylation on Ca^{2+} efflux.

The role of specific PMCA isoforms in the nervous system is largely unknown. We found that PMCA4 contributed significantly to Ca^{2+} efflux after phosphorylation by PKC and thus may play a special role in translating extracellular signals into Ca^{2+}-dependent events within neurons. In contrast, PMCA2 is more active than PMCA4 at basal $[Ca^{2+}]_i$ (Elwess et al., 1997), consistent with the idea that this pump is important for maintaining resting $[Ca^{2+}]_i$. Another feature of PMCA4b is its carboxy-terminal PDZ binding domain that may allow the pump to be clustered with other receptors, transporters, and signaling molecules at specific membrane regions within a neuron (Kim et al., 1998). This may make facilitation of Ca^{2+} efflux by PKC more dramatic within these microdomains relative to that observed in recordings from the bulk cytoplasm. PKC-dependent modulation of PMCA4b in sensory neurons demonstrates how the functional specialization of PMCA isoforms provides precise temporal control of $[Ca^{2+}]_i$ signals in neurons.

PMCAs and Neuronal Function

The significance of PMCAs to neuronal function has only recently become appreciated. Genetic suppression of certain PMCA isoforms can disrupt neuronal differentiation (Brandt et al., 1996) or lead to hearing and balance deficits (Kozel et al., 1998; Street et al., 1998). Here we found that modulation of PMCA-mediated Ca^{2+} efflux controlled the duration of the AHP following a train of action potentials. The slow AHP is generated by Ca^{2+}-activated K^+ channels (Sah, 1996) and is responsible for the slowing of firing rate known as spike frequency adaptation (Hille, 1992). Bradykinin shortened the AHP by accelerating Ca^{2+} efflux, an effect that could account for its ability to reduce spike-frequency adaptation in DRG neurons (Cordoba-Rodriguez et al., 1999). The increased excitability and loss of spike frequency adaptation produced by bradykinin underlies sensitization of peripheral nociceptors. ATP sensitizes DRG neurons to touch and heat, and the PMCA-mediated shortening of the AHP described here may contribute to these excitatory responses (Nakamura and Strittmatter, 1996; Tominaga et al., 2001).

The presynaptic location of PMCAs (Juhaszova et al., 2000; Zenisek and Matthews, 2000), their participation in $[Ca^{2+}]_i$ regulation at axonal release sites (Figures 3 and 5), and their colocalization with voltage-gated Ca^{2+} channels (Hillman et al., 1996) imply that modulation of Ca^{2+} pumps may regulate neurotransmitter release. The high affinity of PMCAs for Ca^{2+} may enable them to play an important role in controlling residual Ca^{2+} and delayed neurotransmitter release. The extent and direction of the changes in Ca^{2+} efflux is determined by the specific PMCA isoforms present at the release site.

Conclusions

We have shown that a specific PMCA isoform is stimulated by neuromodulators. Thus, Ca^{2+} pumps play a more dynamic and specialized role in neuronal function than their previously ascribed role as mere housekeepers of $[Ca^{2+}]_i$ homeostasis. Modulation of Ca^{2+} efflux was found to control excitability in DRG neurons and could potentially affect many processes sensitive to basal $[Ca^{2+}]_i$ and the duration of $[Ca^{2+}]_i$ transients. The heterogeneous distribution of PMCA isoforms differing in their sensitivity to modulation suggests that Ca^{2+} pumps create local domains tuned to specific signaling needs.

Experimental Procedures

Cell Culture

Rat DRG neurons were grown in culture as described (Werth and Thayer, 1994). DRG neurons with cell body diameters of 18–27 μm were used within 2–3 days after plating unless indicated otherwise. For cocultures, spinal neurons were isolated as previously described (Abrahams et al., 1999) and mixed with DRG neurons (1:1) before plating onto laminin-coated coverslips. Cocultures were grown in equal parts DRG and spinal neuron media.

$[Ca^{2+}]_i$ Measurements and Patch-Clamp Recordings

$[Ca^{2+}]_i$ recordings from single DRG neurons using indo-1 or fura-2-based microfluorimetry and whole-cell patch-clamp recordings were performed as described (Jin et al., 1994; Usachev and Thayer, 1999). To image $[Ca^{2+}]_i$ in axons, dye was introduced into single neurons via patch pipettes (0.5 mM). Cells were held in the whole-cell configuration for 3 min, the pipette withdrawn, and recordings made 1–1.5 hr later. Patch pipettes (2–4 MΩ) were filled with the following solution: 125 mM KGluconate, 10 mM KCl, 3 mM Mg-ATP,

1 mM $MgCl_2$, 10 mM HEPES, 0.08 mM indo-1 (pH 7.25 with KOH, 290 mOsm/kg with sucrose). For perforated patch recordings, the pipette contained: 135 mM KGluconate, 10 mM NaCl, 10 mM HEPES, 200 μg/ml amphotericin B (pH 7.25 with KOH, 290 mOsm/kg). Extracellular recording solution contained: 140 mM NaCl, 5 mM KCl, 1.3 mM $CaCl_2$, 0.4 mM $MgSO_4$, 0.5 mM $MgCl_2$, 0.4 mM KH_2PO_4, 0.6 mM Na_2HPO_4, 3 mM $NaHCO_3$, 10 mM HEPES, 10 mM glucose (pH 7.35 with NaOH, 310 mOsm/kg with sucrose). To evoke action potentials in intact neurons, extracellular field stimulation was employed (Werth et al., 1996). Exponential functions were fitted to the data using a nonlinear, least-squares curve fitting algorithm (Origin 4.1 software). Data are presented as mean ± SEM.

Particle-Mediated Gene Transfer to DRG Neurons

Gene transfer into DRG neurons was performed using a biolistic particle delivery system as previously described (Usachev et al., 2000). Mammalian expression plasmids (pCI-neo) harboring cDNAs encoding human PMCA4 splice variant a (hPMCA4a) and nucleotides 71–443 of PMCA4 in the antisense orientation (AS4) were generated as described (Garcia et al., 2001). For hPMCA4a, the full-length cDNA (obtained from Dr. J.T. Penniston, Mayo Clinic) was first cut with Asp718, blunted, and the insert released with SalI and cloned in pCI-neo as described (Garcia et al., 2001). GFP-hPMCA4b was constructed by inserting the entire hPMCA4b coding sequence of a PCR-generated XhoI fragment into pEGFP-C1 (Clontech). The pCI-neo-based constructs were mixed in a 4:1 ratio with a plasmid encoding enhanced green fluorescent protein (pEGFP-C1, Clontech) and precipitated on 1.6 μm gold particles. After 48 hr, transfected cells were identified by green fluorescence (excitation = 480[10] nm, emission = 540[25] nm).

Immunocytochemistry

DRG neurons were fixed with 4% paraformaldehyde in phosphate-buffered saline (PBS) for 15 min at 22°C and rinsed with Ca^{2+}- and Mg^{2+}-free PBS. Cells were treated with PBS containing 0.1% Triton X-100 and 1% rabbit serum for 30 min at 22°C and then incubated overnight with primary antibody at 4°C. PMCA4-selective monoclonal mouse antibodies JA3 and JA9 (Caride et al., 1996) were used at 1:200 or 1:400 dilutions and were a generous gift from Dr. J.T. Penniston. After washing in PBS, cells were incubated with tetramethylrhodamine isothiocyanate (TRITC)-labeled rabbit anti-mouse antiserum (DAKO, Denmark) at a 1:400 dilution for 30 min at 22°C. For synaptophysin labeling, cells were fixed and permeabilized by incubating for 5 min in methanol at −20°C. For colabeling with GFP and PMCA4b-GFP, a mouse monoclonal antibody (Boehringer Mannheim) was used at 0.5 μg/ml, and for colabeling with JA9, a rabbit polyclonal antibody was used (1:250; DAKO). TRITC-labeled donkey anti-mouse or donkey anti-rabbit serum was used as secondary antibody. After washing in PBS, coverslips were inverted on slides over a drop of fluoromount-G (Southern Biotechnology Associates, Birmingham, AL). TRITC (excitation = 568; emission = 605[16] nm) and GFP (excitation = 488; emission = 522[16] nm) labeled neurons were imaged using an Olympus AX70 microscope equipped with the Bio-Rad MRC 1024 laser-scanning confocal imaging system and a 60× objective (NA = 1.40).

Western Blot Analysis

Cells were plated onto laminin-free 60 mm plastic Petri dishes and grown in the presence of cytosine β-D-arabinofuranoside (AraC; 5 μM) for 6 days to obtain enriched neuronal DRG cultures. To provide trophic support for this glial cell-deficient culture, fresh culture medium was mixed with an equal volume of medium conditioned by DRG cultures grown in the absence of AraC for 4–6 days. These growth conditions did not alter $[Ca^{2+}]_i$ homeostasis (n = 3) and yielded cultures containing 73% ± 2% neurons (four independent experiments) as determined using neuron-specific versus total cell labeling (Wang et al., 1998). The cells were washed twice with ice-cold HBS (10 mM KCl, 150 mM NaCl, 50 mM HEPES [pH 7.2]), collected in 1.5 ml HBS, and spun at 8,000 rpm for 5 min at 4°C in a desktop microfuge. Pellets were washed twice with ice-cold HBS and lysed in 2× Laemmli buffer containing a cocktail of protease inhibitors and 5 mM urea, but lacking dyes or reducing agents. The sample was boiled for 2 min, and insoluble material was pelleted by centrifuging for 5 min at 13,000 × g. Samples were analyzed by Western blot as described (Usachev et al., 2001).

Reagents

Indo-1, indo-1 AM, fura-2 AM, and Pluronic F-127 were obtained from Molecular Probes (Eugene, OR). GF109203x, Ro31-8220, and PDBu were obtained from Calbiochem (San Diego, CA). All other reagents were purchased from RBI/Sigma (St. Louis, MO).

Acknowledgments

We thank Kevin Wickman and Ed McClesky for comments on the manuscript; Ali Khammanivong, Wenna Lin, and Kyle Baron for excellent technical assistance; and Adelaida Filoteo and John Penniston for the generous gift of anti-PMCA antibodies. The National Science Foundation (IBN0110409) and the National Institutes of Health (AG16678, DA07304, DA09293, DC04200, GM58710) supported this work.

Received April 20, 2001; revised November 2, 2001.

References

Abrahams, L.G., Reutter, M.A., McCarson, K.E., and Seybold, V.S. (1999). Cyclic AMP regulates the expression of neurokinin1 receptors by neonatal rat spinal neurons in culture. J. Neurochem. *73*, 50–58.

Balasubramanyam, M., and Gardner, J.P. (1995). Protein kinase C modulates cytosolic free calcium by stimulating calcium pump activity in Jurkat T cells. Cell Calcium *18*, 526–541.

Benham, C.D., Evans, M.L., and McBain, C.J. (1992). Ca^{2+} efflux mechanisms following depolarization evoked calcium transients in cultured rat sensory neurones. J. Physiol. *455*, 567–583.

Boyer, J.L., Romero-Avila, T., Schachter, J.B., and Harden, T.K. (1996). Identification of competitive antagonists of the P2Y1 receptor. Mol. Pharmacol. *50*, 1323–1329.

Brandt, P.C., Sisken, J.E., Neve, R.L., and Vanaman, T.C. (1996). Blockade of plasma membrane calcium pumping ATPase isoform I impairs nerve growth factor-induced neurite extension in pheochromocytoma cells. Proc. Natl. Acad. Sci. USA *93*, 13843–13848.

Burgess, G.M., Mullaney, I., McNeill, M., Dunn, P.M., and Rang, H.P. (1989). Second messengers involved in the mechanism of action of bradykinin in sensory neurons in culture. J. Neurosci. *9*, 3314–3325.

Carafoli, E. (1994). Biogenesis: plasma membrane calcium ATPase: 15 years of work on the purified enzyme. FASEB J. *8*, 993–1002.

Caride, A.J., Filoteo, A.G., Enyedi, A., Verma, A.K., and Penniston, J.T. (1996). Detection of isoform 4 of the plasma membrane calcium pump in human tissues by using isoform-specific monoclonal antibodies. Biochem. J. *316*, 353–359.

Cesare, P., Dekker, L.V., Sardini, A., Parker, P.J., and McNaughton, P.A. (1999). Specific involvement of PKC-epsilon in sensitization of the neuronal response to painful heat. Neuron *23*, 617–624.

Cook, S.P., Vulchanova, L., Hargreaves, K.M., Elde, R., and McCleskey, E.W. (1997). Distinct ATP receptors on pain-sensing and stretch-sensing neurons. Nature *387*, 505–508.

Cordoba-Rodriguez, R., Moore, K.A., Kao, J.P.Y., and Weinreich, D. (1999). Calcium regulation of a slow post-spike hyperpolarization in vagal afferent neurons. Proc. Natl. Acad. Sci. USA *96*, 7650–7657.

Dray, A., and Perkins, M. (1993). Bradykinin and inflammatory pain. Trends Neurosci. *16*, 99–104.

Elwess, N.L., Filoteo, A.G., Enyedi, A., and Penniston, J.T. (1997). Plasma membrane Ca^{2+} pump isoforms 2a and 2b are unusually responsive to calmodulin and Ca^{2+}. J. Biol. Chem. *272*, 17981–17986.

Enyedi, A., Verma, A.K., Filoteo, A.G., and Penniston, J.T. (1996). Protein kinase C activates the plasma membrane Ca^{2+} pump isoform 4b by phosphorylation of an inhibitory region downstream of the calmodulin-binding domain. J. Biol. Chem. *271*, 32461–32467.

Enyedi, A., Elwess, N.L., Filoteo, A.G., Verma, A.K., Paszty, K., and Penniston, J.T. (1997). Protein kinase C phosphorylates the a forms

of plasma membrane Ca^{2+} pump isoforms 2 and 3 and prevents binding of calmodulin. J. Biol. Chem. *272*, 27525–27528.

Filoteo, A.G., Elwess, N.L., Enyedi, A., Caride, A., Aung, H.H., and Penniston, J.T. (1997). Plasma membrane Ca^{2+} pump in rat brain—patterns of alternative splices seen by isoform-specific antibodies. J. Biol. Chem. *272*, 23741–23747.

Garcia, M.L., Usachev, Y.M., Thayer, S.A., Strehler, E.E., and Windebank, A.J. (2001). Plasma membrane calcium ATPase plays a role in reducing Ca(2+)-mediated cytotoxicity in PC12 cells. J. Neurosci. Res. *64*, 661–669.

Ghosh, A., and Greenberg, M.E. (1995). Calcium signaling in neurons: molecular mechanisms and cellular consequences. Science *268*, 239–247.

Hille, B. (1992). Ionic Channels of Excitable Membranes (Sunderland, MA: Sinauer Associates).

Hillman, D.E., Chen, S., Bing, R., Penniston, J.T., and Llinas, R. (1996). Ultrastructural localization of the plasmalemmal calcium pump in cerebellar neurons. Neuroscience *72*, 315–324.

Jin, W.Z., Lee, N.M., Loh, H.H., and Thayer, S.A. (1994). Opioids mobilize calcium from inositol 1,4,5-trisphosphate-sensitive stores in NG108-15 cells. J. Neurosci. *14*, 1920–1929.

Juhaszova, M., Church, P., Blaustein, M.P., and Stanley, E.F. (2000). Location of calcium transporters at presynaptic terminals. Eur. J. Neurosci. *12*, 839–846.

Kessler, F., Habelt, C., Averbeck, B., Reeh, P.W., and Kress, M. (1999). Heat-induced release of CGRP from isolated rat skin and effects of bradykinin and the protein kinase C activator PMA. Pain *83*, 289–295.

Kim, E., DeMarco, S.J., Marfatia, S.M., Chishti, A.H., Sheng, M., and Strehler, E.E. (1998). Plasma membrane Ca^{2+} ATPase isoform 4b binds to membrane-associated guanylate kinase (MAGUK) proteins via their PDZ (Psd-95/Dlg/Zo-1) domains. J. Biol. Chem. *273*, 1591–1595.

Kosk-Kosicka, D., and Zylinska, L. (1997). Protein kinase C and calmodulin effects on the plasma membrane Ca^{2+}-ATPase from excitable and nonexcitable cells. Mol. Cell. Biochem. *173*, 79–87.

Kozel, P.J., Friedman, R.A., Erway, L.C., Yamoah, E.N., Liu, L.H., Riddle, T., Duffy, J.J., Doetschman, T., Miller, M.L., Cardell, E.L., and Shull, G.E. (1998). Balance and hearing deficits in mice with a null mutation in the gene encoding plasma membrane Ca^{2+}-ATPase isoform 2. J. Biol. Chem. *273*, 18693–18696.

Krizaj, D., and Copenhagen, D.R. (1998). Compartmentalization of calcium extrusion mechanisms in the outer and inner segments of photoreceptors. Neuron *21*, 249–256.

Miller, R.J. (1991). The control of neuronal Ca^{2+} homeostasis. Prog. Neurobiol. *37*, 255–285.

Nakamura, F., and Strittmatter, S.M. (1996). P2Y1 purinergic receptors in sensory neurons: contribution to touch-induced impulse generation. Proc. Natl. Acad. Sci. USA *93*, 10465–10470.

Ralevic, V., and Burnstock, G. (1998). Receptors for purines and pyrimidines. Pharmacol. Rev. *50*, 413–492.

Sah, P. (1996). Ca(2+)-activated K+ currents in neurones: types, physiological roles and modulation. Trends Neurosci. *19*, 150–154.

Schwiening, C.J., Kennedy, H.J., and Thomas, R.C. (1993). Calcium hydrogen exchange by the plasma membrane Ca-ATPase of voltage-clamped snail neurons. Proc. R. Soc. Lond. Ser. B Biol. Sci. *253*, 285–289.

Stauffer, T.P., Guerini, D., and Carafoli, E. (1995). Tissue distribution of the four gene products of the plasma membrane Ca^{2+} pump. A study using specific antibodies. J. Biol. Chem. *270*, 12184–12190.

Street, V.A., McKee-Johnson, J.W., Fonseca, R.C., Tempel, B.L., and Noben-Trauth, K. (1998). Mutations in a plasma membrane Ca^{2+}-ATPase gene cause deafness in deafwaddler mice. Nat. Genet. *19*, 390–394.

Strehler, E.E., and Zacharias, D.A. (2001). Role of alternative splicing in generating isoform diversity among plasma membrane calcium pumps. Physiol. Rev. *81*, 21–50.

Stucky, C.L., Thayer, S.A., and Seybold, V.S. (1996). Prostaglandin E2 increases the proportion of neonatal rat dorsal root ganglion neurons that respond to bradykinin. Neuroscience *74*, 1111–1123.

Svichar, N., Shmigol, A., Verkhratsky, A., and Kostyuk, P. (1997). ATP induces Ca^{2+} release from IP3-sensitive Ca^{2+} stores exclusively in large DRG neurones. Neuroreport *8*, 1555–1559.

Thayer, S.A., Perney, T.M., and Miller, R.J. (1988). Regulation of calcium homeostasis in sensory neurons by bradykinin. J. Neurosci. *8*, 4089–4097.

Thomas, D., and Hanley, M.R. (1994). Pharmacological tools for perturbing intracellular calcium storage. Methods Cell Biol. *40*, 65–89.

Tominaga, M., Wada, M., and Masu, M. (2001). Potentiation of capsaicin receptor activity by metabotropic ATP receptors as a possible mechanism for ATP-evoked pain and hyperalgesia. Proc. Natl. Acad. Sci. USA *98*, 6951–6956.

Usachev, Y.M., and Thayer, S.A. (1999). Ca^{2+} influx in resting rat sensory neurones that regulates and is regulated by ryanodine-sensitive Ca^{2+} stores. J. Physiol. *519*, 115–130.

Usachev, Y.M., Khammanivong, A., Campbell, C., and Thayer, S.A. (2000). Particle-mediated gene transfer to rat neurons in primary culture. Pflugers Arch. *439*, 730–738.

Usachev, Y.M., Toutenhoofd, S.L., Goellner, G.M., Strehler, E.E., and Thayer, S.A. (2001). Differentiation induces up-regulation of plasma membrane Ca^{2+}-ATPase and concomitant increase in Ca^{2+} efflux in human neuroblastoma cell line IMR-32. J. Neurochem. *76*, 1756–1765.

Verma, A.K., Paszty, K., Filoteo, A.G., Penniston, J.T., and Enyedi, A. (1999). Protein kinase C phosphorylates plasma membrane Ca^{2+} pump isoform 4a at its calmodulin binding domain. J. Biol. Chem. *274*, 527–531.

Wang, K.K.W., Du, Y.S., Diglio, C., Tsang, W., and Kuo, T.H. (1991). Hormone-induced phosphorylation of the plasma membrane calcium pump in cultured aortic endothelial cells. Arch. Biochem. Biophys. *289*, 103–108.

Wang, K.K.W., Villalobo, A., and Roufogalis, B.D. (1992). The plasma membrane calcium pump: a multiregulated transporter. Trends Cell Biol. *2*, 46–51.

Wang, G.J., Chung, H.J., Schnuer, J., Pratt, K., Zable, A.C., Kavanaugh, M.P., and Rosenberg, P.A. (1998). High affinity glutamate transport in rat cortical neurons in culture. Mol. Pharmacol. *53*, 88–96.

Werth, J.L., and Thayer, S.A. (1994). Mitochondria buffer physiological calcium loads in cultured rat dorsal root ganglion neurons. J. Neurosci. *14*, 348–356.

Werth, J.L., Usachev, Y.M., and Thayer, S.A. (1996). Modulation of calcium efflux from cultured rat dorsal root ganglion neurons. J. Neurosci. *16*, 1008–1015.

Yamoah, E.N., Lumpkin, E.A., Dumont, R.A., Smith, P.J.S., Hudspeth, A.J., and Gillespie, P.G. (1998). Plasma membrane Ca^{2+}-ATPase extrudes Ca^{2+} from hair cell stereocilia. J. Neurosci. *18*, 610–624.

Zenisek, D., and Matthews, G. (2000). The role of mitochondria in presynaptic calcium handling at a ribbon synapse. Neuron *25*, 229–237.